Springer

KSME

Journal of Mechanical Science and Technology 24 (9) (2010) 1865~1873
www.springerlink.com/content/1738-494x
DOI 10.1007/s12206-010-0609-8

A simple smart wing actuator using Ni-Ti SMA †

Sanghaun Kim[1] and Maenghyo Cho[2,*]

[1]*Technical Research Laboratories, POSCO, Gwangyang-si, 545-090, Korea*
[2]*WCU Multiscale Mechanical Design Divison, School of Mechanical and Aerospace Engineering, Seoul National University, Seoul, 151-742, Korea*

(Manuscript received November 13, 2009; revised May 7, 2010; accepted May 19, 2010)

Abstract

One way shape memory effect (SME) is not sufficient in the application of the automatic repeated actuation of the SMA wire because the actuator using SME cannot return to its initial shape after it cools down. In the present study, the two-way SME under residual stress is considered. An actuator using the two-way effect of SMA returns to its initial shape by increasing or decreasing the temperature of SMA under initial residual stress. Using the two-way effect, we manufactured a simple smart wing actuator which consists of the SMA wire and a torsional spring to induce variable residual stresses. The SMA wire after the specific training procedure in order for the actuator to be used for the repeated actuations without performance deteriorations in the specified actuation requirements was used. The simple smart wing actuator has been tested for repeated actuations in still-air as an environmental thermal condition for the practical aspect of its usage. The characteristics of actuator behavior according to operation thermal cycle duration time, i.e., the response characteristics for rapid actuation were investigated. By the application of the simple smart wing actuator using the SMA wire, SMA shows novel performance in repeated actuations.

Keywords: SMA; Residual stress; Two-way SME; Thermal cycle time; Actuator

1. Introduction

A shape memory alloy (SMA) experiences a large transformation strain (typically ranging from 2 to 10%) by inducing stress and generates a large recovery force to volume (or power to weight) when it is heated by shape memory effect under residual stress. An SMA is commonly heated by giving an electric current. Also, the phase transformation temperatures of an SMA can be shifted by infinitesimally changing the composition ratio of Ni and Ti (As matter of fact, it is known that NiTi alloys must have a composition of 49/51 at.% Ni - Bal. Ti). Using these characteristics of SMA, we can control the shape or suppress specific vibration modes of structures. Therefore, SMA wires and patches are frequently used as active components in smart structures. Their ability to provide large recovery forces and displacements has been useful in various engineering applications, including devices for controlling the shapes of spaceship antennas, aircraft wings, and submarine sterns or the vibrations of host structures [1-3]. In the present study, we focus on the repeated actuation of the system. We make experimental investigation on the characteristics of the actuation behavior of SMA wires for practical application without performance deteriorations.

The generation of a large strain resulting in a large force is one of the main requirements in actuation performance. SMAs can achieve this workable strain by phase transformation. There are two ways in transforming the phase of SMAs - one, by changing the temperature of SMAs, i.e., temperature-induced martensite (TIM) transformation and the other, by applying stresses on SMAs, i.e., stress-induced martensite (SIM) transformation. These two transformations cause a strong thermo-mechanical coupling behavior in the material. Four different temperatures are specified for the phase transformation by temperature change: martensite finishing (M_f), starting (M_s), austenite starting (A_s) and finishing temperatures (A_f). Phase transformation is accomplished by each phase of starting or finishing temperature. These temperatures are strongly stress-dependent. Stress-inducing at a given environmental temperature causes phase transformation from the austenite/twinned martensite phase to the detwinned martensite phase. In this process, the phase transformation process of SMAs is similar to the deformation process in plasticity. But in the phase transformation of SMA, it should be emphasized that the transformation (yield) stresses of SMA strongly depend on the temperature of SMA. In other words, transformation stresses vary as the temperature of SMA changes.

SMAs are inherently non-linear actuators exhibiting significant hysteresis in their stress–strain–temperature characteris-

† This paper was recommended for publication in revised form by Associate Editor Jeong Sam Han

*Corresponding author. Tel.: +82 2 880 1693, Fax: +82 2 886 1693
E-mail address: mhcho@snu.ac.kr

tics. The transformation upon heating/cooling and the transformation upon loading/unloading do not overlap each other. Thus, SMA actuators exhibit hystereses and their behavior is very sensitive to the interactions of those characteristics, i.e., these two hysteresis behaviors occur simultaneously when SMA is used in actuators. Thus it is difficult to predict the behavior of the actuators precisely by considering these two kinds of hysteresis behaviors.

In this paper, we manufactured a simple smart wing actuator that consists of an SMA wire for actuation and torsional spring to induce variable residual stresses. Here, the SMA wire after the specific training procedure in order for the actuator to be used for the repeated actuations without performance deteriorations in the specified actuation requirements was used. The actuation test was performed, which contains not only a simple repeated actuation test but also a test for the thermal rate effect according to the thermal cycle times. All the experimental tests were performed in still-air condition of room temperature and it might have some experimental errors because the environment of the SMA wire was not thermally isolated. But it is quite common that the actuators made of SMA wire are exposed to the air. The effect of this external environment should be considered carefully for the practical aspect of its usage. This kind of actuator can be applied to the air-vehicle wing/flap and air inlet/outlet.

2. Design of the simple smart wing actuator and experimental setup

We manufactured a simple smart wing actuator as shown in Fig. 1 (schematic) and Fig. 2 (real view) and performed the actuation test. The actuator consisted of the SMA wire and torsion spring, load-cell, laser displacement sensor, displacement controller, rotation shaft and rotation angle measurement device. NACA0012 model is used as the airfoil shape.

The torsional spring was mounted on the rotation axis to give residual stress to the SMA wire. Here, one end of torsional spring is clamped at the rotation shaft and the other end is fixed at the body (frame). The torsional spring has a stiffness (torsional spring constant) of 3.07N/deg, which is measured at the 22.03mm deviatoric point from its center. SMA wire was attached to the rotation shaft at one end and the other end was connected to the displacement controller and load-cell which is attached to the frame. The load-cell which has the rated capacity of 20Kgf measures the force (stress) of the SMA wire during operation. The displacement controller could change the initial residual stress of the SMA wire, because this displacement controller draws the SMA wire by adjusting the screw. The temperature was measured at the mid-point of the SMA wire by using a K-type thermocouple. To check a temperature profile along the direction of wire length, five equally located thermocouples at the SMA wire were used. The rotation angle of the wing and the displacement of the SMA wire were measured by laser displacement sensor, which is an optical displacement measuring device in a non-contact manner and then calculated, by using rotation

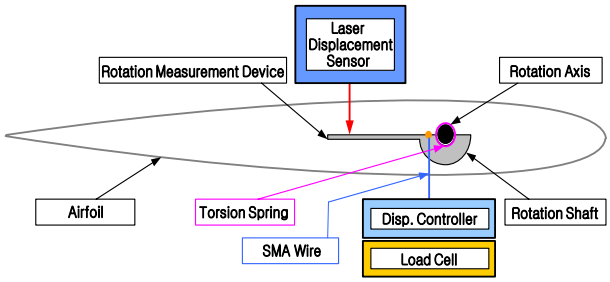

Fig. 1. The schematic of simple smart wing actuator for experimental test.

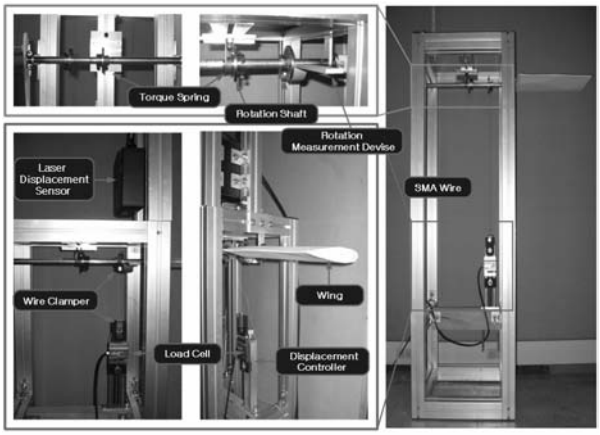

Fig. 2. The real view of simple smart wing actuator for experimental test.

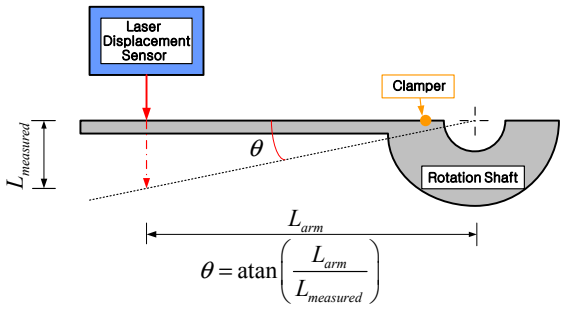

Fig. 3. The rotation measuring device & the way to calculate the rotation angle.

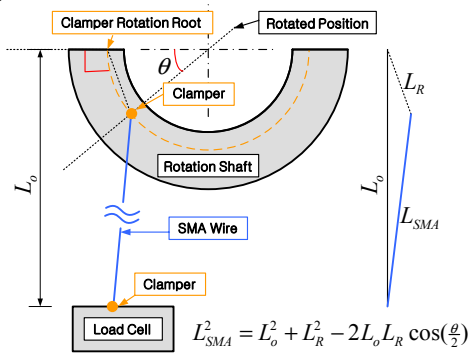

Fig. 4. The way to calculate the deformed SMA wire length.

measurement device from the calculation method of Fig. 3 and Fig. 4, respectively. In the actuation mechanism of this actuator, the angle of attack of simple smart wing was changed as the SMA wire was contracted in the heating process and released in the cooling process.

3. Experimental tests

In this study, the Ni-Ti SMA wire was obtained from Diado Steel Corporation. The nominal composition of the SMA wire employed was 53.3Ni-46.7Ti, all numbers given in wt%, from the electron probe X-ray micro analyzer (EPMA). We used the 0.361mm-diameter SMA wire initially untrained (as-received). And it was annealed (heat treatment) above a critical temperature, which has been shown to result in a single stage martensite transformation without any R-phase. The austenite finishing temperature (A_{of}) of the SMA wire was about 20℃ at the stress-free state, which was measured by DSC (differential scanning calorimetry) method. First, to minimize the accumulation of plastic strain generated by repeated actuations, which causes a performance deterioration of the actuator using as-received SMA initially, the SMA wire was trained thermally by applying 500 cycles with 60 second thermal cycle time under 65.97N (6.732kg) and in the temperature range between 20℃ and 130℃. Through this thermal training, the SMA wire showed the same trajectory in constitutive behavior in repeated actuation due to the saturation of permanent deformation (plastic strain or irreversible martensite variants) and transformation stresses/temperatures [4-9]. This training is compatible with the purpose of usage of the presented actuator. After training, the diameter of SMA wire became 0.348mm. The SMA wire was then heated above 100℃ at the stress-free state to eliminate the residual martensite phase. Using a programmable DC power supply, electrical current was applied from 0 to 1.3 Ampere with time, and then cooled down to room temperature by ambient temperature (still-air), to have the temperature distribution according to time in the heating and cooling process as symmetric as possible. Here, maximum 1.3 Ampere was chosen for heating the SMA wire above about 120℃.

Before the actuation test, we performed the tension (loading-unloading) test of the thermally trained SMA wire by using INSTRON 5565^{TM} at different temperatures between 0 to 50℃ to evaluate the initial residual force (or stress of SMA wire) of the actuator. This tension test was conducted at 0.01/min strain rate. The test result is shown in Fig. 5. The shape memory behavior appeared below about 30℃ and pseudoelastic behavior appeared above this temperature. When the tensile stress, which is approximately equal to 450 MPa, is induced to the SMA wire at room temperature (22℃), the phase of the wire was fully transformed with detwinned martensite variants. In addition, the four transformation stresses and temperatures were shifted by thermal training compared to those of the untrained SMA wire, because plastic strains or irreversible martensite variants during the material

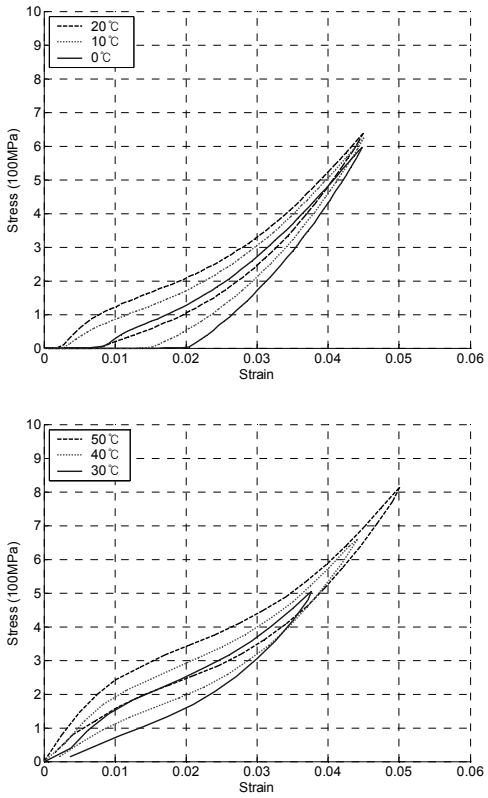

Fig. 5. The stress-strain curves of trained SMA wire from tension test: Shape Memory Effect (Upper) and Pseudoelasticity (Lower).

training change the material substructure and then shift the material characteristics and properties of SMA material [4-9].

The initial (unstressed, unforced) SMA wire length was 314.6mm-long, which was measured when the rotation measurement device which is attached to the wing and parallel to its chord was parallel to ground. The displacement controller was used to apply a residual stress of 450MPa to the SMA wire. This residual stress was large enough to make full phase transformation by stress-inducing at room temperature (22℃). In this state, the initial strain was approximately 0.036, which was exactly the same strain as shown in Fig. 5. Also, the strain contained a two-way strain, 3.4%, that is generated by thermal cycle on the residual stress. The initial rotation angle was about 15° in pre-actuation state. The rotation angle was calculated by the trigonometric function as shown in Fig. 3. The deformed SMA wire length was calculated by the second law of cosine, which is given in Fig. 4. Here, the distance between the center of axis and the clamped point for wire at the rotation shaft was 22.03mm. The change of angle is increased as this distance is decreased. But an actuation force is increased and therefore, an actuation temperature range is increased as this distance is decreased. Therefore, in order to determine the above-mentioned distance, we should consider the several requirement parameters of the actuator such as a range of change of angle of attack, range of operating stress/temperature, capacity of power supply for maximum heated temperature, and so on. The engineering strain and its conjugate stress

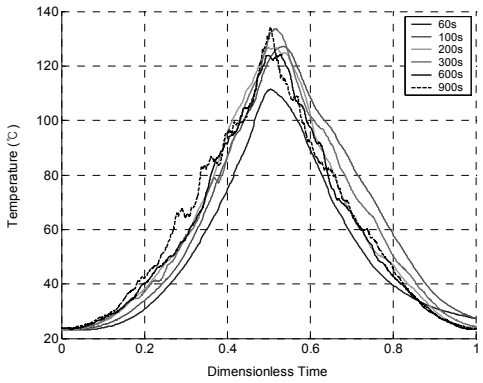

Fig. 6. The temperature-dimensionless time curves according to thermal cycle times.

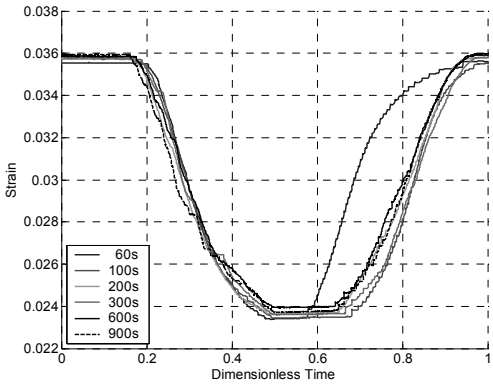

Fig. 7. The strain-dimensionless time curves according to thermal cycle times.

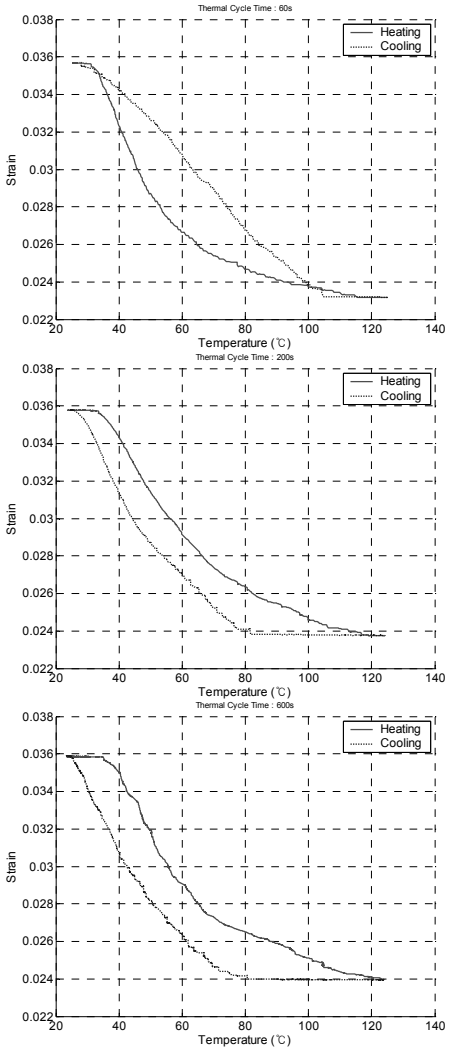

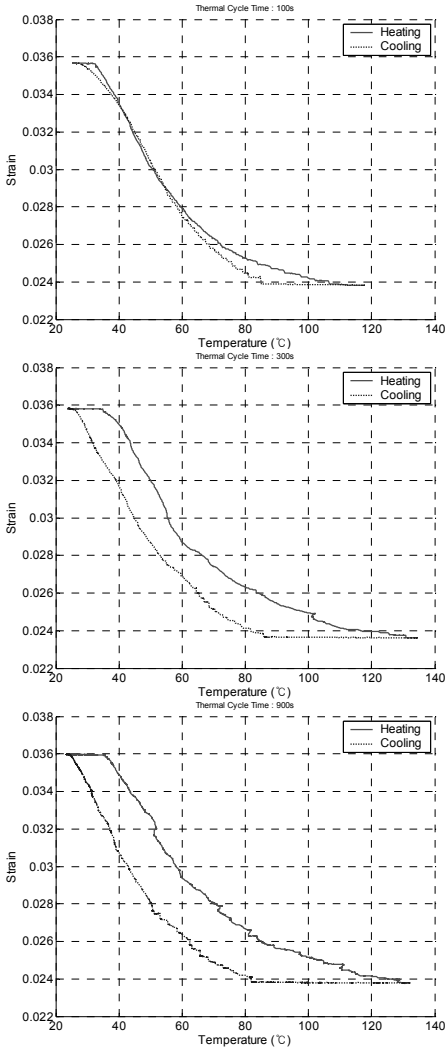

Fig. 8. The strain–temperature curves according to thermal cycle times.

measure with respect to the training complete state are used in the present work.

Experimental tests were conducted for various thermal cycle time rates that are 60, 100, 200, 300, 600, 900 second/cycle to investigate the characteristics of actuator behavior according to the thermal cycle time, i.e., the response characteristics for rapid actuation. Here, each thermal rate is generated by the programmable DC power supply that can change the elapse-time per cycle for the aforementioned applying electric current (0~1.3A). The electric current with time is given to SMA wire with symmetry in each thermal cycle time. For each thermal rate, the tests were performed and the results

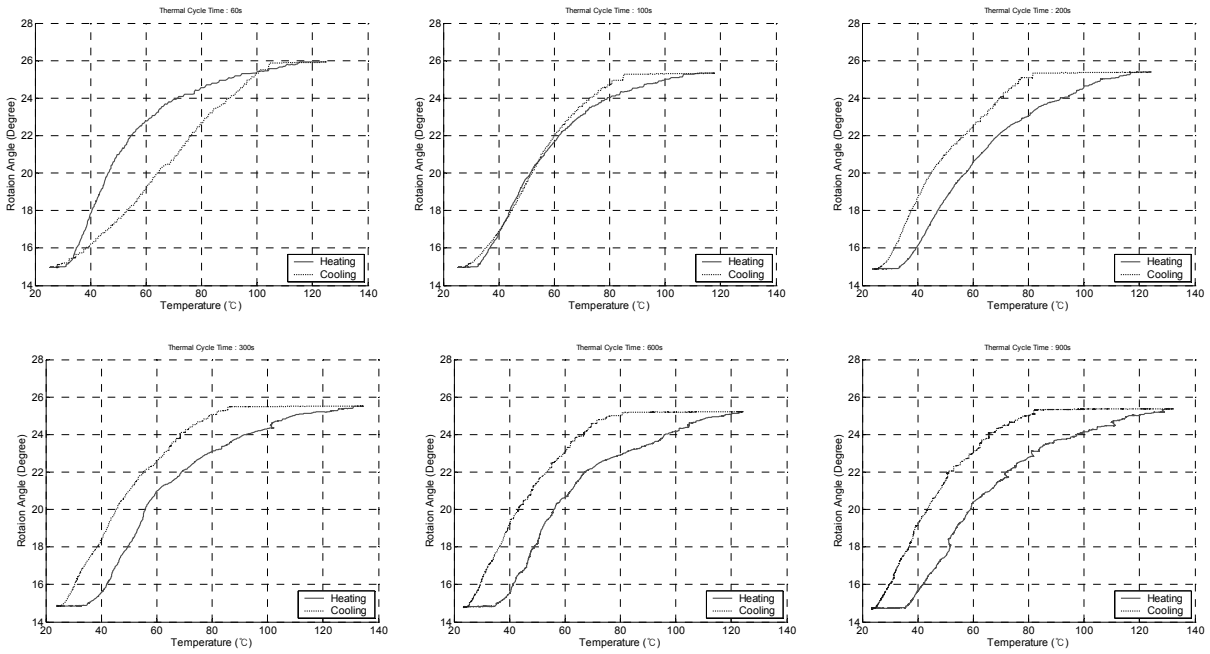

Fig. 9. The rotation angle–temperature curves according to thermal cycle times.

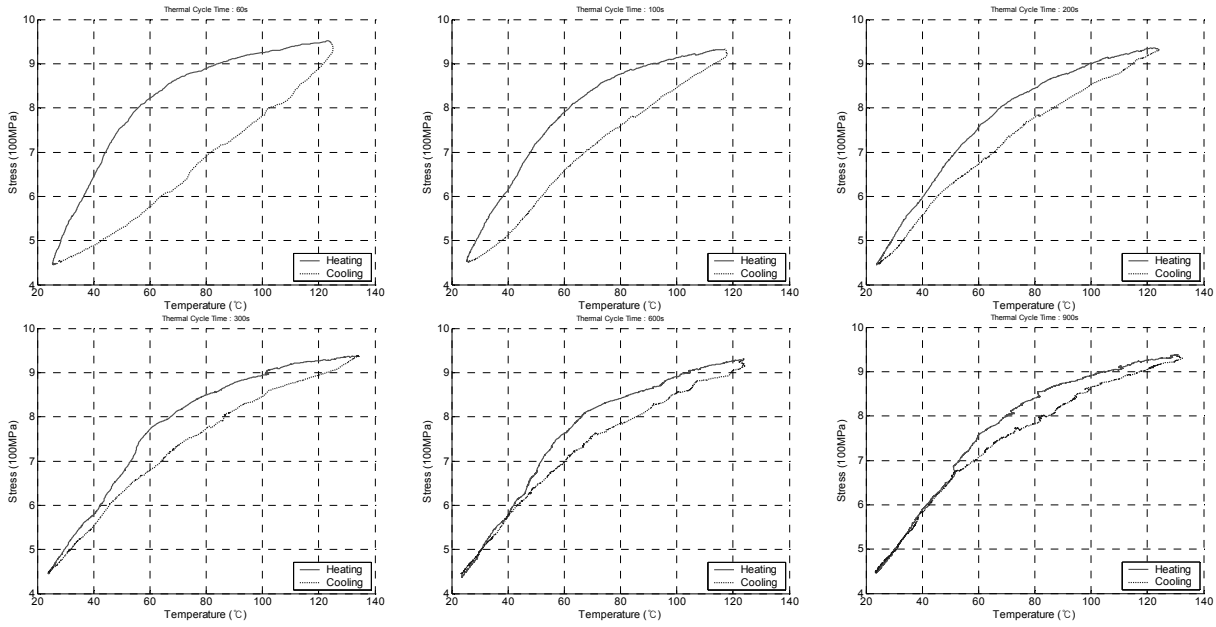

Fig. 10. The stress–temperature curves according to thermal cycle times.

of complete three cycles were averaged. Because the wire temperature cannot drop down to room temperature by the natural cooling below 60 second/cycle, the above-measured cycle time-rates greater than 60 seconds were selected.

4. Results and discussion

Figs. 6 and 7 show the wire mid-point temperature and total strain change of the SMA wire with respect to the non-dimensional time in which each thermal cycle time is normalized to unity, respectively. In the fast thermal cycle case (60sec/cycle), the temperature cannot be increased greatly due to the lack of time to heat the wire sufficiently. The temperature distribution is not symmetric along the time axis, i.e., the fast thermal cycle case showed a slower temperature gradient with time than the other cases of thermal cycle time, which can be described by the ohmic resistance heating lag of heating region. From the above reasons, Fig. 7 shows that the actuator was recovered much more in the case of fast thermal cycle time at the same dimensionless time point during cooling, because a sufficient temperature level could not be sustained. Especially, in the cooling region of 60 second thermal

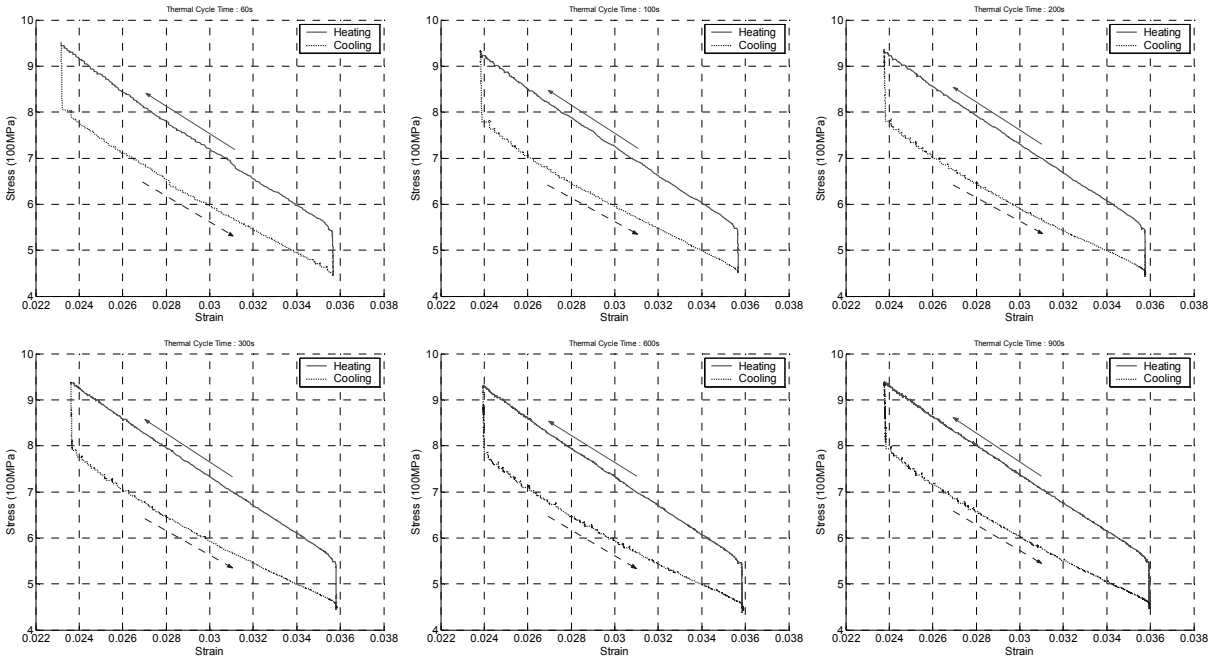

Fig. 11. The stress–strain curves according to thermal cycle times.

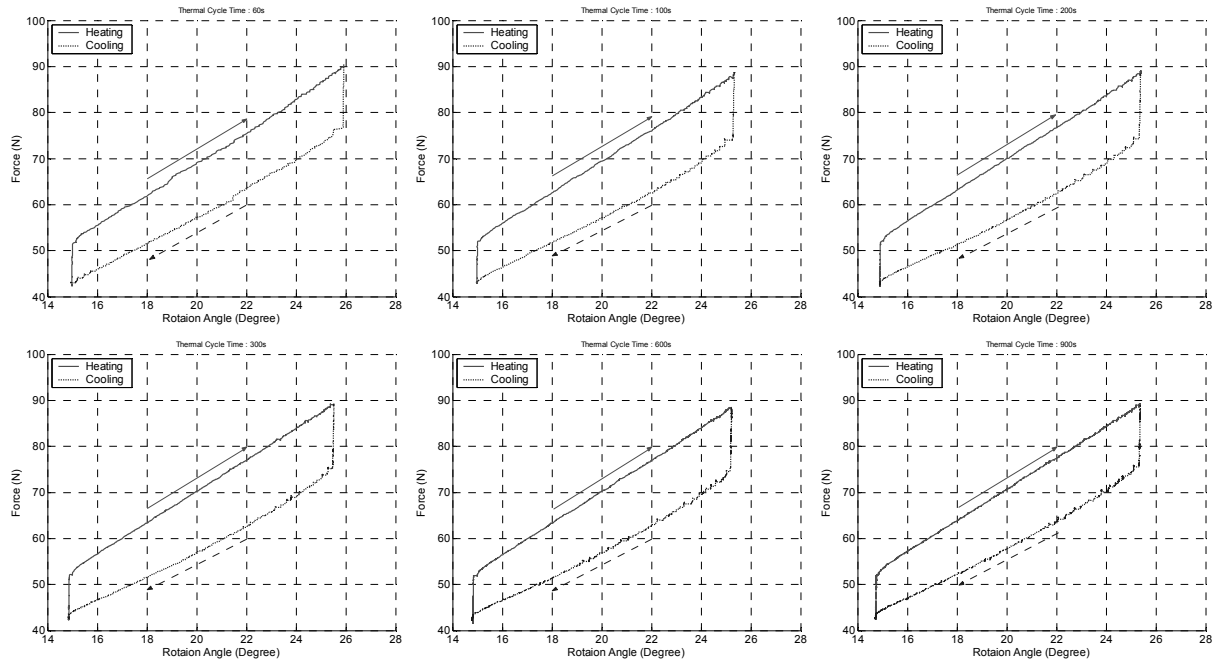

Fig. 12. The force–rotation angle curves according to thermal cycle times.

cycle time, the wire temperature is influenced more by the natural cooling of the air then ohmic resistance heating. Thus, in the cooling region of this fast rate case, the transformation strain was more generated by force than those in other cases of slower thermal cycle times. In 100 second thermal cycle time, a little ohmic resistance heating lag occurred. But, above 200 second thermal cycle time, the whole temperature distribution to the reference time is symmetry due to the sufficient time for heating and cooling.

Figs. 8-13 show the strain–temperature, rotation angle–temperature, stress–temperature, stress–strain, force–rotation angle and stress–strain–temperature curves of the actuator at various thermal cycle times, respectively.

From the given electrical current, the generated actuation temperature ranged between 25℃ to 130℃ (Fig. 6). The two-way (transformation) strain change of the SMA wire was about 1.2% (Fig. 7 and 8). The change of the rotation angle was about 10.5 ° (Fig. 9). The change of the stress during ac-

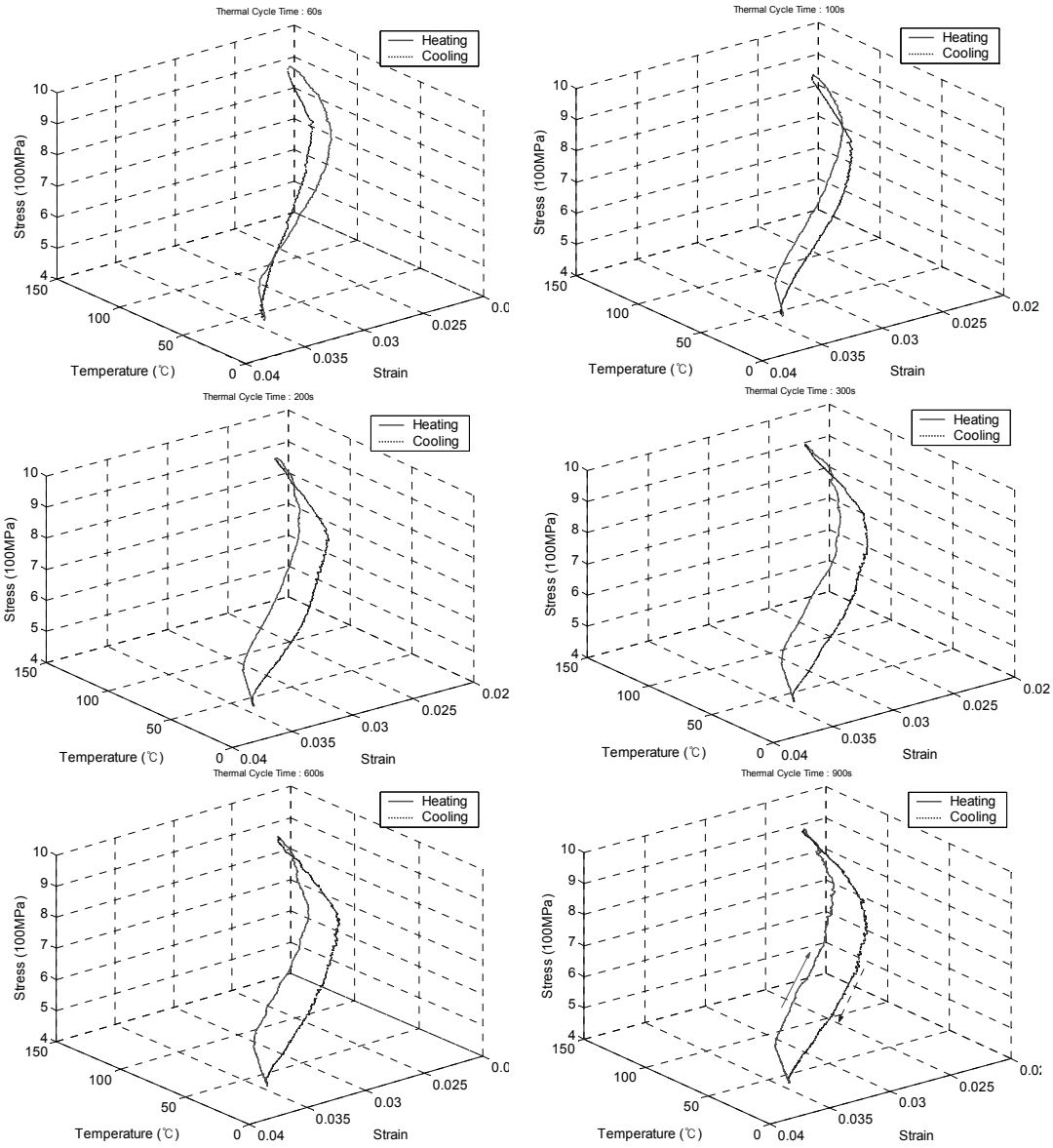

Fig. 13. The strain–temperature–stress curves according to thermal cycle times.

tuation was about 470MPa (Fig. 10).

In the strain–temperature curves of Fig. 8, as the thermal cycle time increases from 60 second/cycle, the hysteresis becomes smaller and the trajectory path moves along the counter-clockwise direction. Around 100-second thermal cycle time, hysteresis nearly disappears. Above the 100-second thermal cycle time, the hysteresis in the thermal cycles becomes wider and the thermal cycle path changes from the counter-clockwise direction to the clockwise direction. Above the 600-second thermal cycle time, hysteresis is almost unchanged. This phenomenon occurs mainly because the temperature profile along the direction of the wire length with time during heating differs from that during cooling.

But, the direction of the thermal cycle path of the stress–temperature curve (Fig. 10) does not change, and the hysteresis of the stress–temperature curve becomes smaller. Because of the temperature profile given in the direction of the SMA wire length and variable force (stress) condition during heating/cooling process, the transformation strain by loading/unloading (SIM transformation) is introduced locally near both sides of the wire which has a relatively low temperature. But, in the interior region of the wire, the TIM transformation is dominant. This phenomenon due to hysteresis existence can be explained in the stress–strain curves in Fig. 11, too. If the temperature is uniformly distributed along the entire length of the wire or the local inspection for non-uniform distributed temperature can be given, the stress–temperature curve would be similar to the rotation angle–temperature curve (Fig. 9). Also, the stress–strain (Fig. 11) and force–rotation angle (Fig. 12) curve will not have hysteresis during actuation. The actuation behavior and direction cannot be characterized as given in Fig. 8. In addition, as the thermal cycle time increases, the

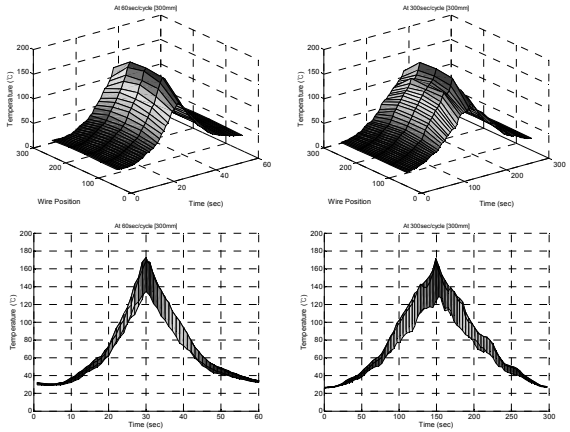

Fig. 14. The temperature-time curves according to thermal cycle times [60s (Left), 300s (Right)].

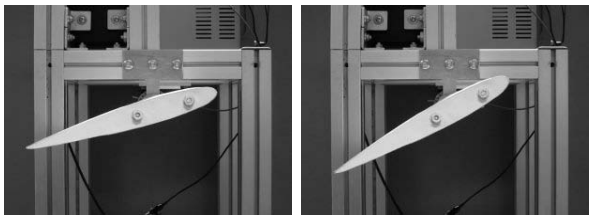

Fig. 15. The initial (Left) and maximum (Right) actuated shape of simple smart wing actuator.

temperature profile along the direction of the wire length with time will stabilize the SMA wire to be in a certain state, in which the pattern of the hysteresis behavior is not changed.

The reason for the thermal rate effect of SMA wire seems to be the effect of thermal profile along the SMA wire length with time. This thermal profile with time is formed by heat conduction/convection to its external environment, and this thermal distribution causes the non-uniform deformation (or strain distribution) to the SMA wire. In this test, the temperature is measured at the mid-point of the wire and the length change of entire SMA wire length is measured globally. Therefore, it is considered that the thermal rate effect appears due to non-uniform thermal distribution along the length of SMA wire with time according to the thermal cycle time. The thermal profile along the wire length with time at the heating process is different from that of cooling process at a fast thermal rate. If temperature and displacement are measured at several points of SMA wire along the axial direction, the rate effect can be more clearly understood. For these, with the generated temperature range from 25 to 170°, the rate test was conducted with 60-second and 300-second thermal cycle time (Fig. 14). In the 60-second case, the temperature profile along the direction of wire length with time in the heating process is remarkably different from that in cooling process. But, in the 300-second case, the temperature profile with time is almost the same as that in the heating and cooling process. Here, for checking a temperature profile along the direction of wire length with time, the five equally located thermocouples at the SMA wire were used.

Stress–strain relations (Fig. 11) and force–rotation angles relations (Fig. 12) are nearly the same and they have no dependency on the thermal cycle time. The subtle difference in these figures is attributed to the scattering of the generated temperature at each test. The transformation strain is not fully recovered in the actuator due to both the temperature profile along the wire length with time and the variable force during actuations. To maximize the recovery of the transformation, uniform temperature along the wire length with time should be maintained.

Fig. 15 shows the initial (left) and maximal actuated (right) shape of simple smart wing actuator.

5. Conclusion

We manufactured a simple smart wing actuator working at the ground (still-air) environment and performed an actuation test. For this repetitively working actuator which has the same actuation trajectory, the SMA wire was trained thermally in the practical operating range of temperature and under practical maximum stress level. The experimental actuation test was performed at the room temperature, but had some difficulties in predicting the actuator behavior due to the temperature profile along the wire length with time, which is a function of thermal cycle time and spatial location. Because the SMA wire is utilized in still-air, it must be carefully handled to consider the effect of this ambient thermal condition for the practical aspect of its usage.

From the experimental tests of the simple smart wing actuator, the following results were observed. For the repetitively working actuation having same trajectory, an SMA must be trained to satisfy the specified actuation requirements of actuator. If rapid cooling is applied to the system, the actuation time can be reduced. If a proper temperature profile along the wire length with time for the cycling rate is given to the SMA wire, the actuation hysteresis can be removed. Then, the behavior prediction of the SMA may be further simplified since a complicated hysteresis does not have to be considered. And the operating control systems of actuator using SMA can be constructed easily. To fix and find a certain shape or position of actuator can be included in these operating controls.

The application of a simple smart wing actuator using the SMA wire showed the novel performance of the SMA wire in the repeated actuations. This kind of actuator has high potential in application to the aircraft wing/flap and air in-let/out-let.

6. Future work

From the above experimental results and numerical algorithm for smart structures [10, 11], we will predict the behavior of a simple smart wing actuator according to thermal cycle time through more experimental tests in which the temperature profile along the wire length with time will be measured. It is difficult to simulate the behavior of an actuator that has

simultaneously contracted and released phase transformation strains due to thermal and mechanical loading/unloading within the material, which has not been reported. The numerical algorithm for this kind of actuator simulation is required to analyze the complicated thermally and mechanically combined phase transformation behavior.

Acknowledgment

This work was supported by the Korea Science and Engineering Foundation (KOSEF) grant funded by the Korean government (MOST) (No. R0A-2009-000-20109-0) and also supported by WCU (World Class University) program through the Korea Research Foundation funded by the Ministry of Education, Science, and Technology (R31-2009-000-10083-0)

References

[1] K. Otsuka and C.M. Wayman, *Shape Memory Materials*, Cambridge University Press, UK (1999).
[2] T. Waram, *Actuator Design Using Shape Memory Alloys*, Second Ed. Mondotronics Inc., UK (1993).
[3] V. Birman, Review of mechanics of shape memory alloy structures, *Appl. Mech. Rev.*, 11 (1997) 629-645.
[4] S. Kim, H. Choi, M. Yoon and M. Cho, Experimental test for numerical simulation SMA characteristics and its simulation, *in: Smart Structures and Materials, Proc. of SPIE*, 6170, San Diego, USA (2006).
[5] B. Erbstoeszer, B. Armstrong, M. Taya and K. Inoue, Stabilization of the shape memory effect in NiTi: An experimental investigation, *Scripta Mater.*, 42 (2000) 1145-1150.
[6] H. Scherngell and A. C. Kneissl, Training and stability of the Intrinsic two-way shape memory effect in Ni-Ti alloys, *Scripta Mater.*, 39 (1998) 205-212.
[7] H. Tobushi, Y. Shimeno, T. Hachisuka and K. Tanaka, In fluence of strain rate on superelastic properties of NiTi shape memory alloy, *Mechanics of Materials*, 30 (1998) 141-150.
[8] H. C. Lin, S. K. Wu and J. C. Lin, The martensitic transformation in Ti-rich TiNi shape memory alloys, *Materials Chemistry and Physics*, 37 (1994) 184-190.
[9] Y. Liu and P. G. McCormick, Factors Influencing the Development of Two-Way Shape Memory in NiTi, *Acta Metallurgica et Materialia*, 38 (7) (1990) 1321-1326.
[10] M. Cho and S. Kim, Structural morphing using two-way shape memory effect of SMA, *Int. J. Solids and Struc.*, 42 (2005) 1759-1776.
[11] S. Kim and M. Cho, Numerical simulation of double SMA wire actuator using two-way shape memory effect of SMA, *Smart Mater. Struc.*, 16 (2007) 372-381.

Maenghyo Cho received a Ph. D degree from the University of Washington in 1993. He is currently Professor at School of Mechanical & Aerospace Engineering at Seoul National University, Seoul, Korea. His research interests are multiscale/nano mechanics including MD and DFT simulations and Computational solid/structural mechanics.
Researcher

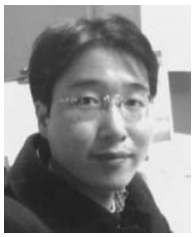

Sanghaun Kim received a Ph. D degree of Mechanical & Aerospace Engineering from Seoul National University. He is currently senior researcher at Auto Steel Application Group in POSCO. His research interest is on developing constitutive equations to simulate nonlinear deformation behavior of smart materials such as shape memory alloy.